Front. Struct. Civ. Eng. 2022, 16(8): 1029–1039
https://doi.org/10.1007/s11709-022-0861-x

RESEARCH ARTICLE

Prediction of characteristic blast-induced vibration frequency during underground excavation by using wavelet transform

Tae Un PAK[a], Guk Rae JO[a], Un Chol HAN[b*]

[a] *Faculty of Mining Engineering, Kim Chaek University of Technology, Pyongyang 999093, Democratic People's Republic of Korea*

[b] *School of Science and Engineering, Kim Chaek University of Technology, Pyongyang 999093, Democratic People's Republic of Korea*

[*] *Corresponding author. E-mail: huch8272@star-co.net.kp*

ABSTRACT Blast-induced vibration produces a very complex signal, and it is very important to work out environmental problems induced by blasting. In this study, blasting vibration signals were measured during underground excavation in carbonaceous shale by using vibration pickup CB-30 and FFT analyzer AD-3523. Then, wavelet analysis on the measured results was carried out to identify frequency bands reflecting changes of blasting vibration parameters such as vibration velocity and energy in different frequency bands. Frequency characteristics are then discussed in view of blast source distance and charge weight per delay. From analysis of results, it can be found that peak velocity and energy of blasting vibration in frequency band of 62.5–125 Hz were larger than ones in other bands, indicating the similarity to characteristics in the distribution band (31–130 Hz) of main vibration frequency. Most frequency bands were affected by blasting source distance, and the frequency band of 0–62.5 Hz reflected the change of charge weight per delay. By presenting a simplified method to predict main vibration frequency, this research may provide significant reference for future blasting engineering.

KEYWORDS wavelet analysis, blast-induced vibration, frequency characteristics, underground excavation

1 Introduction

Drilling and blasting play an important and positive role in the fields of mining and civil engineering [1]. However, blasting can have some negative effects on both mine safety and the surrounding environment, such as airblast, noise, vibration, and flying rocks. In particular, blasting vibration can be the most important factor influencing the safety of civil structures [2–4].

Because blasting vibration is very complex and contains many vibration components of different frequency bands, researches on the influence of blasting vibration have been limited to theoretical analysis, measurement test and numerical simulation for blasting vibration signals [5–10]. Up to now, measured signals of blasting vibration have been analyzed by using Fourier and wavelet transforms, and many studies have focused on determining time−frequency characteristics for blasting vibration signals. Since a Fourier transform consists of a sine wave and its harmonic wave, it has localization characteristics in a single frequency space. Fourier transform can analyze characteristics of signals in time-, space-, and frequency-space but it can't be used in two-dimensional time-frequency space. To overcome this disadvantage, Dennis Gabor proposed a short-delay time Fourier transform, that is, the Gabor transform in 1946 [11]. The Gabor transform overcame the disadvantage of Fourier transform to a certain degree; however, it could not smoothly solve a time-frequency localization problem because the size of the time-frequency window was fixed.

In practice, frequency and time resolutions have to be constantly high for analyzing signal components of low

Article history: Received Nov 5, 2021; Accepted May 14, 2022

frequency and high frequency. This problem could be solved by changing the size of window in response to frequency changes. Morlet, a geophysicist from France, proposed the concept of wavelet transform in the early 1980s [12]. With a detailed study on Gabor transform method, he proposed the concept of the "Morlet wavelet" by clarifying the commonality and distinction relating to an original Fourier transform and a short-delay time Fourier transform, and analyzing their features and functional fabrics. Frequency resolution reduces when analyzing signal components of high frequency, while time resolution reduces when analyzing signal components of low frequency. Therefore, the analysis results for the local features of burst signal by wavelet transform are different each other, so the wavelet transform has been used to detect components of burst signals or to process edge signals. The local feature of wavelet transform in time-frequency space can be widely used in the field of signal processes. In particular, it is suitable to process and analyze signals of which delay time is short and changes quickly [13,14].

On the other hand, the waveforms of vibration induced by blasting of explosive, and consequent signals incident upon a structure, reflect the blasting vibration intensity. Analysis indices, such as peak vibration velocity, main vibration frequency, energy density and so on, are obtained from the waveform, and then, the vibration intensity and blasting efficiency can be estimated. Main vibration frequency depends on the nature of the ground and will decrease as the propagation distance increases [6]. The proportion of high frequency bands in the blasting vibration energy decreases with increase in the amount of an explosive charge. The higher the explosion velocity of explosive is, the more obvious the change rate of ground vibration energy in high frequency band is.

Some researchers have applied wavelet analysis theory to the signal process of blasting vibration to determine the delay time of short-delay blasting, and suggested variation characteristics of blasting vibration frequency [2,3,15,16]. Ainalis et al. [14] analyzed time-frequency distribution characteristics of blasting vibration to determine their main frequency and peak vibration velocity. Besides, wavelet analysis has been widely used to understand the frequency characteristics of blasting vibration by estimating vibration energy characteristics applied to civil structures, identifying time errors during blasting, appreciating vibration characteristics of geological structure and so on [17–22].

In this study, the characteristics of the vibration velocity and energy in different frequency bands and the characteristics of the main vibration frequency in an arbitrary blasting condition were predicted by wavelet analysis for vibration signals induced by blasting of an inclined shaft. First, the blasting vibration signals during excavation of the inclined shaft in carbonaceous shale were measured using a vibration pickup and FFT analyzer. Then, wavelet analysis on the measured results was carried out to identify frequency bands that reflect changes of blasting vibration parameters such as vibration velocity and energy in different frequency bands.

2 Research method

2.1 Wavelet transform

A wavelet transform is a signal processing tool with the ability of analyzing both stationary and non-stationary data, and to produce both time and frequency information with a higher (more than one) resolution. The wavelet transform is used to represent the arbitrary time signal $f(t)$ of linear combinations of wavelet functions [11,12]. For the scale a and time variable b, the continuous wavelet transforms of the signal $f(t) \in L^2(R)$ and its inverse transform are defined as [14,18]:

$$WT_{\mathrm{f}}(a,b) = \langle f(t), \psi_{a,b}(t) \rangle = |a|^{-1/2} \int_{-\infty}^{+\infty} f(t)\psi*\left(\frac{t-b}{a}\right)\mathrm{d}t, \tag{1}$$

$$f(t) = \frac{1}{C_\psi} \int_{0}^{+\infty}\int_{-\infty}^{+\infty} \frac{1}{a^2} WT_{\mathrm{f}}(a,b)\psi\left(\frac{t-b}{a}\right)\mathrm{d}a\mathrm{d}b, \tag{2}$$

where $\langle f(t), \psi_{a,b}(t) \rangle$ is the scalar product of $f(t)$ and $\psi_{a,b}(t)$, $\psi*\left(\frac{t-b}{a}\right)$ is the complex conjugate function of $\psi\left(\frac{t-b}{a}\right)$.

For the wavelet transform, because many signals are discrete sampling signals of which length is limited, a continuous wavelet transform should be discretized. Therefore, reconstructed formulae of a discrete wavelet transform corresponding to $a = a_0^j$, $b = ka_0^j b_0$ $(j \in Z, a_0 > 1)$ can be written as follows:

$$WT_{2^j} f(k) = \langle f(R), \psi_{2^j}(t) \rangle = \frac{1}{2^j} \int_{-\infty}^{+\infty} f(t)\psi*(2^j t - k)\,\mathrm{d}t, \tag{3}$$

$$\begin{aligned} f(t) &= \sum_{j\in Z} WT_{2^j} f(k)\psi_{2^j}(k) \\ &= \sum_{j\in Z} \int WT_{2^2} f(k)\psi_{2^j}(2^{-j}t - k)\,\mathrm{d}k, \end{aligned} \tag{4}$$

where $\psi_{j,k}(t)$ is the discrete wavelet transform, $C_{j,k}$ is the coefficient of discrete wavelet transform and $f(t)$ is the constructed signal.

A blasting vibration signal $f(t)$ can be analyzed by the Mallat algorithm, which decomposes and reconstructs the wavelet transform, as follows:

$$\begin{aligned} f(t) &= A_1(t) + D_1(t) \\ &= A_2(t) + D_2(t) + D_1(t) = \cdots \\ &= A_N(t) + D_N(t) + D_{N-1}(t) + \cdots \\ &\quad + D_2(t) + D_1(t) \end{aligned}$$

$$\Rightarrow f(t) = A_N(t) + \sum_{i=1}^{N} D_i(t). \quad (5)$$

If $A_N(t) = D_0(t)$, Eq. (5) is

$$f(t) = \sum_{i=0}^{N} D_i(t), \quad (6)$$

where $A_i(t)$ and $D_i(t)$ are respectively signal components of low frequency and high frequency bands of blasting vibration signal $f(t)$ in the wavelet decomposed layer of i grade; N is number of total decomposed layers, and i is number of each decomposed layer ($i = 0,1,2,\ldots,N$).

A wavelet transform of a blasting vibration signal allows us to see the vibration characteristic according to duration of vibration signal components of different frequency bands. If blasting vibration signal $f(t)$ is decomposed into N layers, the total energy of vibration signal can be calculated as follows:

$$E = \int_{-\infty}^{+\infty} f(t)^2 \mathrm{d}t = \sum_{i=0}^{N} \int_{-\infty}^{+\infty} D_i(t)^2 \mathrm{d}t + \sum_{m \neq n} \int_{-\infty}^{+\infty} D_m(t) \cdot D_n(t) \mathrm{d}t. \quad (7)$$

Thus, in each frequency band, the energy of blasting vibration signal is calculated by

$$E_0 = \sum_{n=1}^{M} |A_N(n)|^2, \quad (8)$$

$$E_i = \sum_{i=1}^{N} \sum_{n=1}^{M} |D_i(n)|^2, \quad (i = 0,1,2,\ldots,N) \quad (9)$$

where $A_N(n)$ represents low frequency band components of blasting vibration signal obtained by wavelet transform to N layers, and $D_i(n)$ represent high frequency band components of the i layer of the decomposed blasting vibration signal.

Therefore, the total energy of blasting vibration signals is defined as follows:

$$E = E_0 + E_i, \quad (10)$$

where E_0 is the energy of the low frequency band component of the blasting vibration signal obtained by wavelet transform to N layers, $(\mathrm{cm/s})^2$. And E_i is the energy of the frequency band component of i grade, $(\mathrm{cm/s})^2$.

2.2 Blasting vibration measurement

The measuring system of the blasting vibration consists of a vibration pickup CB-30 and FFT analyzer AD-3523. Vibration pickup CB-30, of which the characteristic frequency is 30Hz and sensitivity is 0.17 $\mathrm{V \cdot cm^{-1} \cdot s^{-1}}$, was manufactured in Russia, and FFT analyzer AD-3523 (Fig. 1) was manufactured by A&D CO.LTD in Tokyo, Japan.

The surrounding rock is carbonaceous shale with uniaxial compressive strength of about 35 MPa, containing many cracks between layers and is very soft. The vibration pickup was set up on a side wall away from the driving face of inclined shaft, so that the axis was parallel to the shaft, as shown in Fig. 2.

Blasting vibration signals were measured whenever the vibration pickup was fixed in one site and the driving face was advanced by blasting. The results obtained from different condition of charge weight per delay and blasting source distances are shown in Table 1 and Fig. 3.

3 Predicting frequency characteristics of blasting vibration signals

3.1 Analysis of measured signals

In order to find frequency characteristics of blasting vibration signals, a wavelet transform was used to analyze the measured data. The MATLAB function sym8 is commonly chosen for the analysis of blasting vibration signals. Because characteristic frequency band of common structures was 3–15 Hz, the number of wavelet decomposed layers was chosen to be $N = 5$ to ensure that the band belonged to the minimum frequency band. The sampling frequency of measured blasting vibration signals was 1000 Hz, so the signals included frequency components of 0–500 Hz in accordance with the sampling theorem of Shannon [11].

As the number of decomposed layers of blasting vibration signals was 5, on the basis of signal decomposition theory of Mallat algorithm, the signal was decomposed to six frequency band contents (i.e., 0–15.625, 15.625–31.25, 31.25–62.5, 62.5–125, 125–250, and 250–500 Hz).

Fig. 1 Vibration pickup CB-30 and FFT analyzer AD-3523.

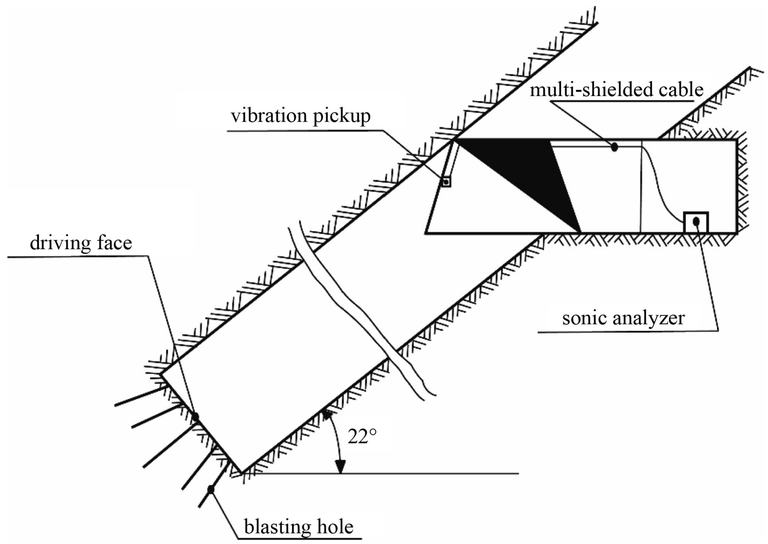

Fig. 2 Measurement condition and setting state of devices.

Table 1 Measuring data of blasting vibration

signal	blasting source distance, R (m)	charge weight per delay, Q_{step} (kg)	total charge weight (kg)	peak vibration velocity, V_{max} (cm/s)
1	2.0	0.2	0.2	5.7471
2	2.0	0.2	0.2	4.1420
3	4.6	0.2	0.6	2.5353
4	5.2	0.4	1.6	4.4471
5	5.2	0.4	1.6	4.2353
6	8.4	0.4	0.4	1.7918
7	8.4	0.2	0.4	1.9524
8	13.9	0.3	0.6	1.1941
9	13.9	0.6	0.6	1.5100
10	14.6	0.6	3.2	1.8770

The frequency band contents of blasting vibration signal 1 obtained by wavelet transform using MATLAB is shown in Fig. 4.

Peak vibration velocity (V_{max}) and energy (E) of frequency bands on ten measured signals are shown in Figs. 5 and 6.

Attenuation of peak vibration velocity (V_{max}) and vibration signal energy (E) with increase of blasting source distance (R) in each frequency band are shown in Figs. 7–10.

Also, in order to consider attenuation of peak vibration velocity and vibration signal energy in each frequency band according to charge weight per delay, three signals at the similar distances from the blasting sources were chosen from Table 1. Then, $Q_{step}-V_{max}$ and $Q_{step}-E$ diagrams were compared with each other, as shown in Figs. 9 and 10.

It can be seen from Figs. 5 and 6 that peak vibration velocity and vibration signal energy have the largest values in 62.5–125 Hz of the frequency band and the main vibration frequency is also within this range. With increase of the distance to blasting source, peak vibration velocities of the signal components in most frequency bands decreased, except in frequency bands (125–250 Hz). That is, the influence of blasting source distance change for peak vibration velocity could be seen in most frequency bands, as shown in Figs. 7 and 8. The increasing tendency of peak vibration velocity with increase of charge weight per delay was identified from velocity curves of other bands in the frequency bands of 0–15.625 and 31.25–62.5 Hz, as shown in Fig. 9. The proportionality of charge weight per delay and vibration signal energy was well reflected in the frequency band of 0–15, 15.625–31.25, and 31.25–62.5 Hz (Fig. 10).

To ensure frequency bands corresponding to influence factors of blasting vibration, the differences of the tendency curves for 31.25–62.5 and 62.5–125.0 Hz from the other four curves indicated in Figs. 9 and 10 were considered as follows; firstly, characteristics of influence factors such as charge quantities and blasting source distance might not be completely reflected in the bands of 31.25–62.5 and 62.5–125.0 Hz, and secondly, some discrepancies exist in assessed factors of blasting vibration with change of influence factors.

3.2 Determination of main vibration frequencies for predicted waveform of blasting vibration

Once waveform of blasting vibration is correctly predicted, not only damping and frequency characteristics of blasting vibration for rock mass and feature of explosion source can be predicted and considered, but also damage and injury induced by blasting vibration can be prevented in advance. Blasting vibration signals directly measured *in situ* can be considered as a function reflecting features of rock mass and blasting conditions, such as physical and mechanical properties and geological structures, propagation properties and the quantity of explosive and so on. Therefore, it can be seen that predicting the blast vibration waveforms under different conditions by using

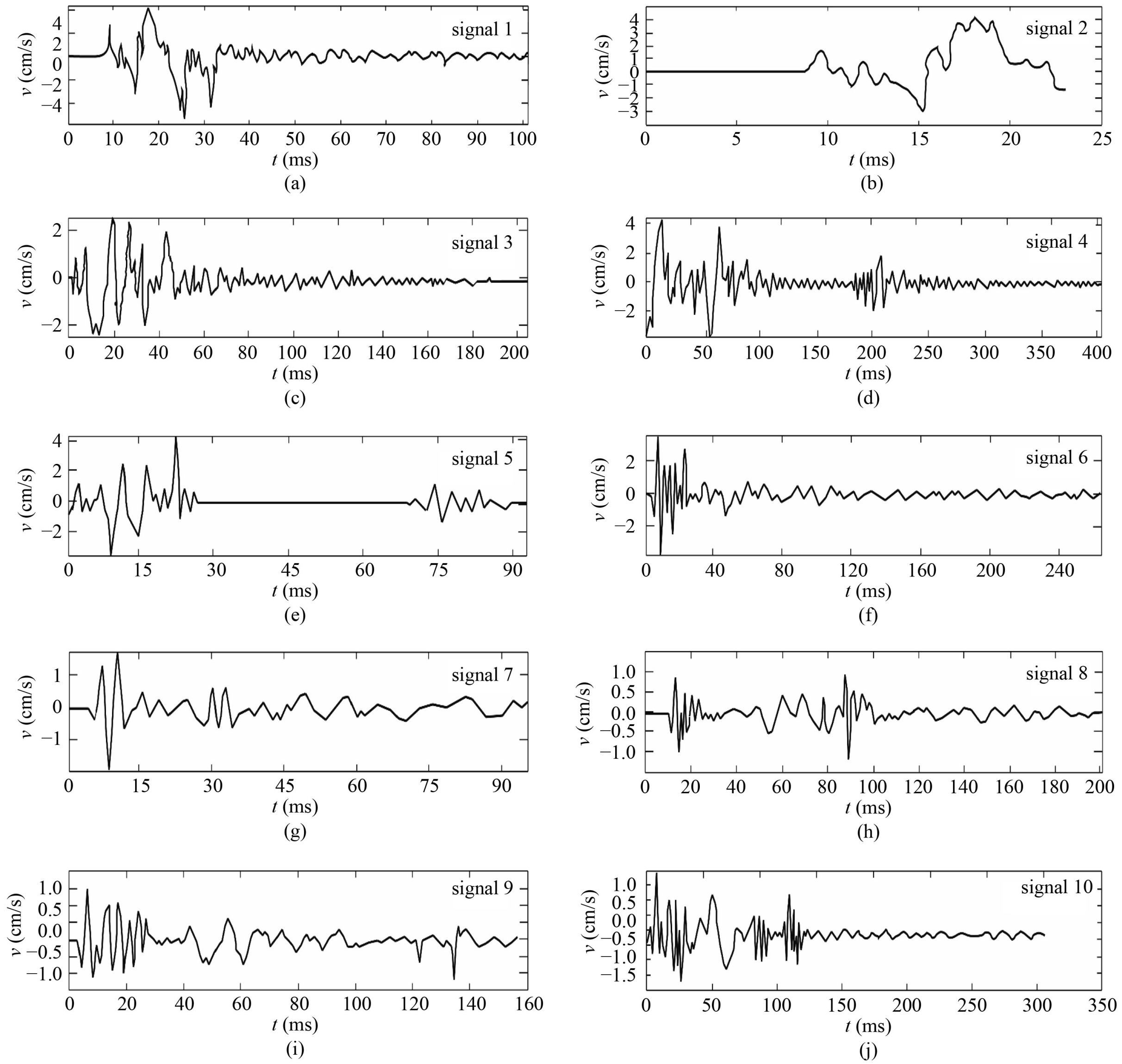

Fig. 3   Waveform of measured blasting vibration. (a) Signal 1; (b) signal 2; (c) signal 3; (d) signal 4; (e) signal 5; (f) signal 6; (g) signal 7; (h) signal 8; (i) signal 9; (j) signal 10.

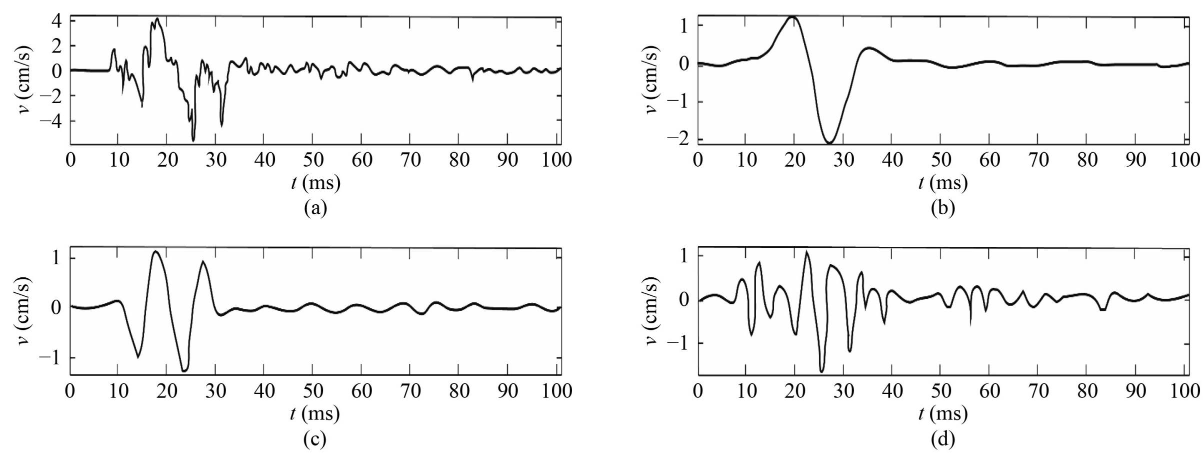

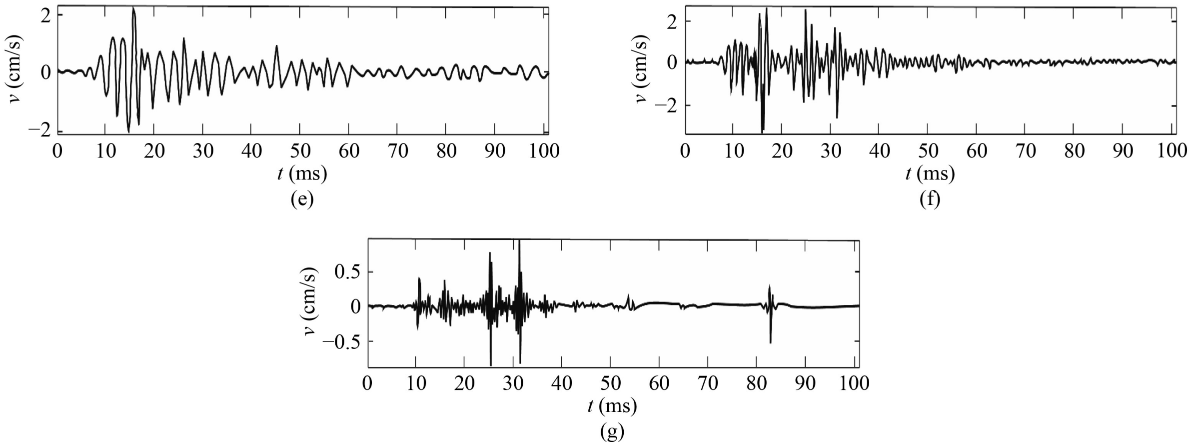

Fig. 4 Blasting vibration contents of six decomposed frequency bands: (a) blasting vibration signal; (b) 0–15.625 Hz frequency band content; (c) 15.625–31.25 Hz frequency band content; (d) 31.25–62.5 Hz frequency band content; (e) 62.5–125 Hz frequency band content; (f) 125–250 Hz frequency band content; (g) 250–500 Hz frequency band content.

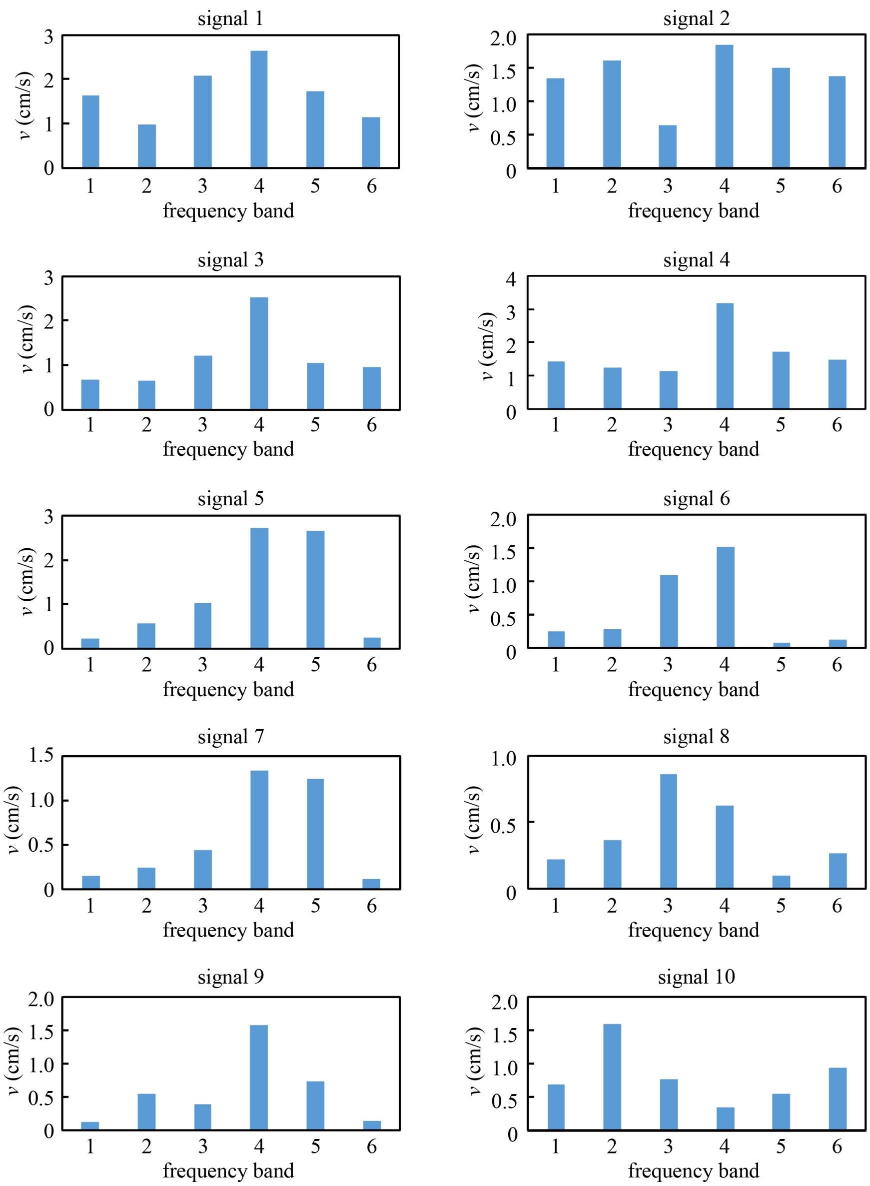

Fig. 5 Peak vibration velocity of blasting vibration components in each frequency band.

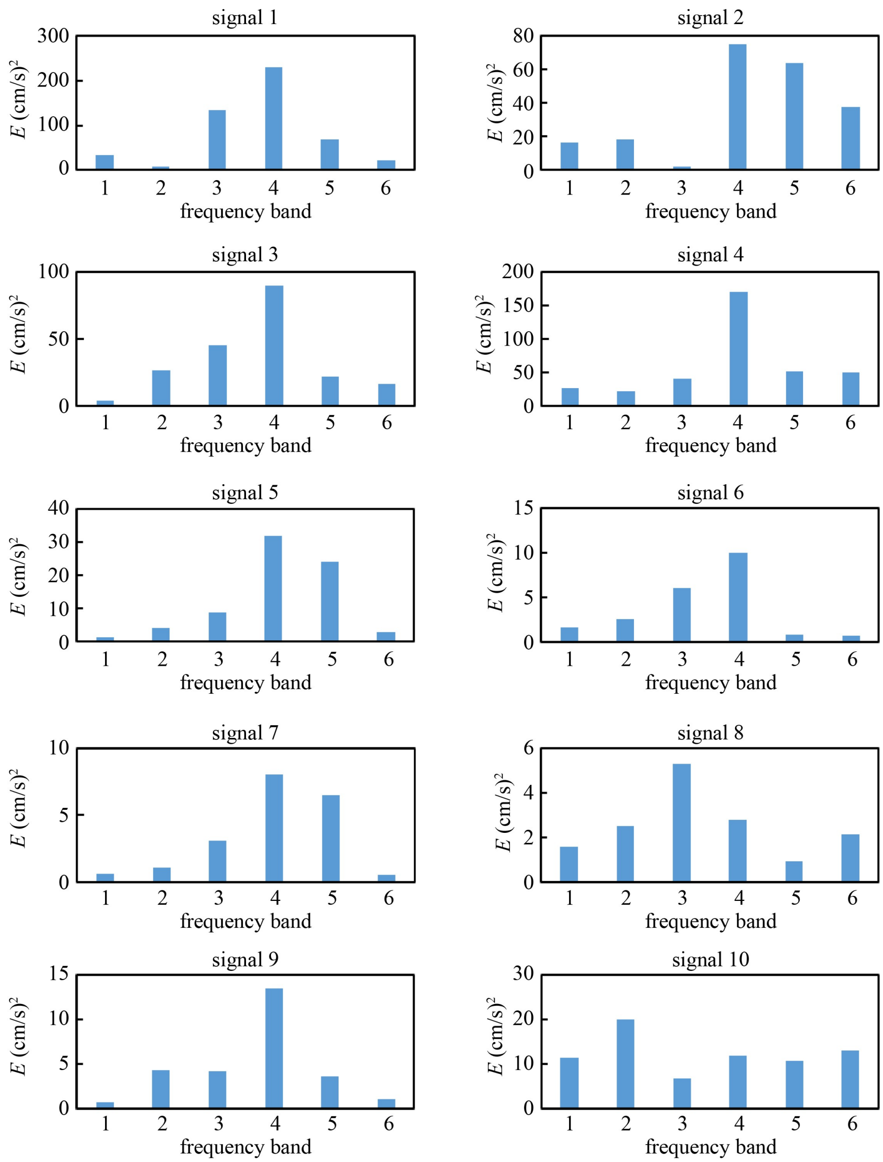

Fig. 6 Energy of blasting vibration components in each frequency band.

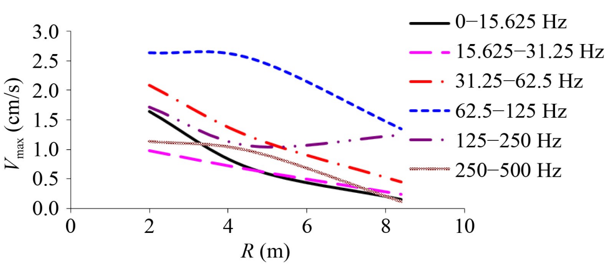

Fig. 7 $R-V_{max}$ diagram of blasting vibration signal components in each frequency band.

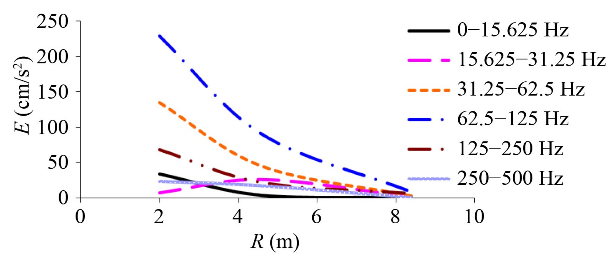

Fig. 8 $R-E$ diagram of blasting vibration signal components in each frequency band.

the primitive function of the actual measured blast vibration signal better reflects the accuracy of the prediction and the characteristics of the blast vibration waveforms compared to the method for predicting the waveform by the synthesis of harmonic waves based on the vibration propagation theory.

In this paper, the theory for signal decomposition and reconstruction of wavelet transform was applied to predict the waveform of blasting vibration. First, by using the theory for signal decomposition of wavelet transform,

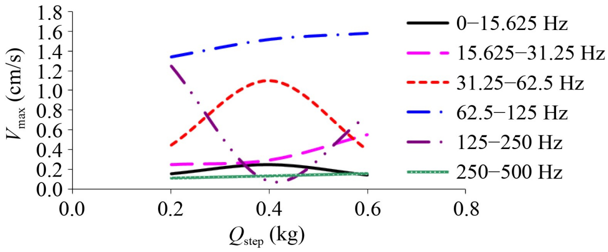

Fig. 9 Q_{step}–V_{max} diagram of blasting vibration signal components in each frequency band.

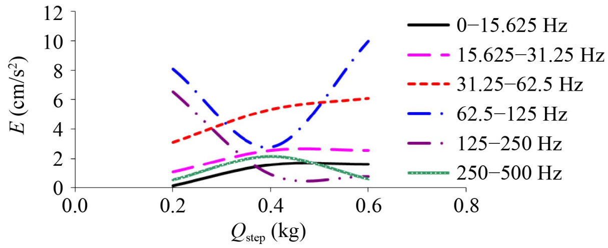

Fig. 10 Q_{step}–E diagram of blasting vibration signal components in each frequency band.

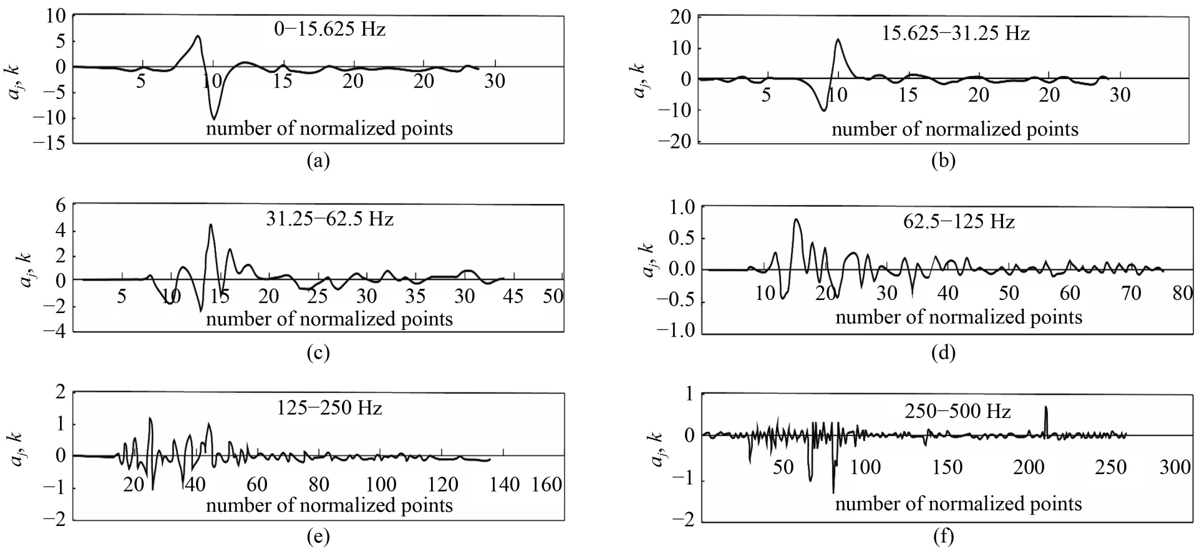

Fig. 11 Normalized wavelet coefficients. (a) 0–15.625 Hz; (b) 15.625–31.25 Hz; (c) 31.25–62.5 Hz; (d) 62.5–125 Hz; (e) 125–250 Hz; (f) 250–500 Hz.

blasting vibration signal selected as primitive function was decomposed to signal components of several frequency bands, and then, wavelet coefficient in each band could be obtained. Blasting vibration signal selected to primitive function can well reflect all conditions and features such as rock mass, blasting conditions and so on. Therefore, wavelet coefficients for each frequency band in different conditions were predicted by normalizing wavelet coefficients of primitive functions and multiplying them according to Eq. (11), below, considering the vibration damping features. Then, wavelet coefficients are predicted by the theory for signal reconstruction of wavelet transform, and signal components of blasting vibration in each frequency band could be predicted using the coefficients. Finally, the waveform of blasting vibration was predicted.

The damping coefficients of k_j and α_j for ten signals of blasting vibration were determined by Eq. (11), which is already well known equation for calculation of blasting vibration velocity, as summarized in Table 2.

$$v_j = k_j \left(\frac{\sqrt[3]{Q}}{R} \right)^{\alpha_j}. \qquad (11)$$

Table 2 Damping coefficients and characteristic equation of blasting vibration components in each frequency band

frequency band (Hz)	k_j	α_j	characteristic equation
0–15.625	1.9345	0.6491	$v_1 = 1.9345\left(\frac{\sqrt[3]{Q}}{R}\right)^{0.6491}$
15.625–31.25	1.1966	0.2652	$v_2 = 1.1966\left(\frac{\sqrt[3]{Q}}{R}\right)^{0.2652}$
31.25–62.5	1.7815	0.3251	$v_3 = 1.7815\left(\frac{\sqrt[3]{Q}}{R}\right)^{0.3251}$
62.5–125	5.8268	0.6005	$v_4 = 5.8268\left(\frac{\sqrt[3]{Q}}{R}\right)^{0.6005}$
125–250	5.3260	0.8898	$v_5 = 5.326\left(\frac{\sqrt[3]{Q}}{R}\right)^{0.8898}$
250–500	2.6116	0.7932	$v_6 = 2.6116\left(\frac{\sqrt[3]{Q}}{R}\right)^{0.7932}$

As shown in Table 2, it can be found that the value of k_j tends to increase when the frequency of blasting vibration components is high, while blasting vibration intensity decreases rapidly with increase of the frequency band of blasting vibration component (i.e., the value of α_j), indicating that damping degree of blasting vibration intensity is defined by the value of α_j. Therefore, attenuations of blasting vibration signals are different from each other in all frequency bands and discreteness of k_j and α_j are comparatively large. Meanwhile, it should be noted that curves simulated from equations v_4 and v_5 listed in Table 2 are slightly different from measured curves, even if these equations were obtained from the tendency curves for 62.5–125 and 125–250 Hz on the basis of measured data. Consequently, Eq. (11) seems not to ideally reflect the characteristics of frequency bands between 62.5 and 250 Hz.

The signal components of blasting vibration of six frequency bands (i.e., 0–15.625, 15.625–31.25, 31.25–62.5, 62.5–125, 125–250, and 250–500 Hz), and their wavelet and sampling coefficients were obtained by selecting signal 1 to the primitive function and performing wavelet transform (Fig. 11). The wavelet coefficients in each frequency band for nine waveforms of blasting vibrations except signal 1 were predicted using sampling wavelet coefficients and damping coefficients of k_j and α_j for blasting vibration in all frequency bands listed in Table 2. Then, the predicted waveforms were compared with measured waveforms of blasting vibrations, as shown in Fig 12.

The main vibration frequency was determined by the wavelet transform for predicted waveforms of blasting vibration signals again, and the result was compared with those of measured waveforms, as shown in Fig. 13.

It can be seen from Fig. 13 that the predicted curve agrees with the measured curve, as the relative error of main vibration frequency is 4.63%.

4 Conclusions

It is very important in blasting engineering that blasting results and structure situation are correctly predicted by analyzing blasting vibration signals obtained in different conditions in situ.

This paper suggested a method for analyzing frequency characteristics of blasting vibration measured in an

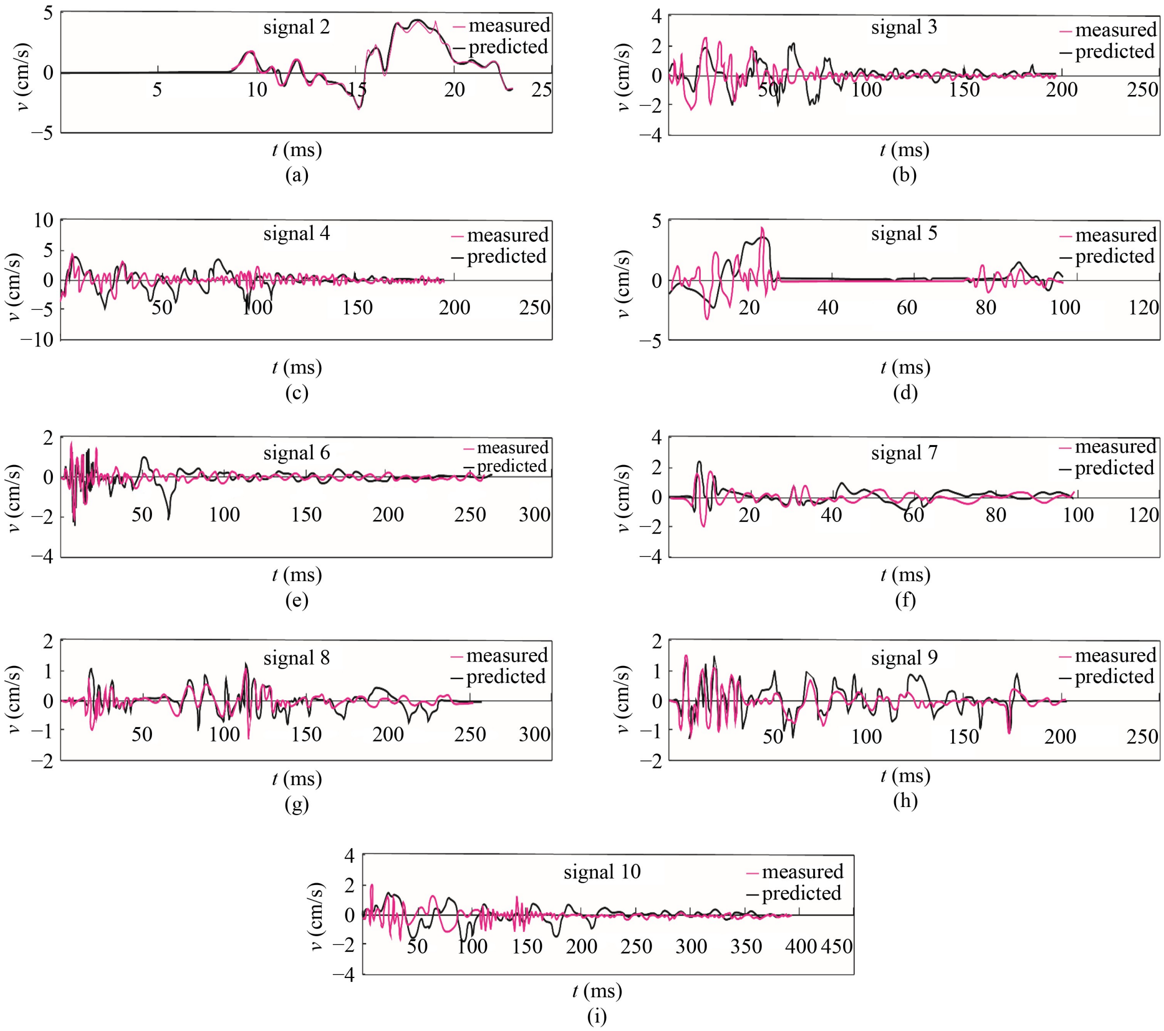

Fig. 12 Comparisons between predicted and measured waveforms. (a) signal 2; (b) signal 3; (c) signal 4; (d) signal 5; (e) signal 6; (f) signal 7; (g) signal 8; (h) signal 9; (i) signal 10.

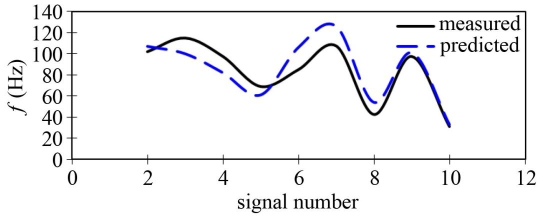

Fig. 13 Comparative analysis of predicted and measured values of main frequency band.

adjacent drift during driving and blasting of an inclined shaft, and for predicting them in different blasting conditions. Main vibration frequency can be confined to the frequency band for which blasting vibration intensity and energy are the largest. Almost of all frequency bands reflected the variation of blasting source distance, while the frequency band of 0–62.5 Hz reflected the variation of charge weight per delay. By performing wavelet transform for blasting vibration signals selected as primitive functions which can reflect physical properties of rock mass, blasting conditions and so on, the frequency characteristics of blasting vibration in the adjacent drift could be predicted with changes of charge quantities and blasting source distance.

In this paper, the signals of blasting vibration were analyzed in the conditions limited to a kind of explosive and geological structure, a limited amount of charge and distance. However, it should be noted that the frequency band wasn't determined by reflecting various situation of charge quantities and blasting source distances, and frequency characteristics of other bands wasn't analyzed enough because the frequency range is too wide. Thus, future work will focus on interpretation of frequency characteristics of blasting vibration for a wide range of charge quantities under different explosives and geological structures, in order to contribute more practically to study and practice of the blasting process and associated environmental protection.

Acknowledgements The authors are grateful for the financial support received from the National Science and Technical Development Foundation of DPRK Korea (No. 24-210301).

References

1. Mishra A K, Gupta R N. Rapid excavation of tunnels using innovative drilling and blasting techniques. In: The 10th International Symposium on Rock Fragmentation by Blasting. London: Tailor & Francis Group, 2013, 15−22
2. Wang Z, Fang C, Chen Y, Cheng W. A comparative study of delay time identification by vibration energy analysis in millisecond blasting. International Journal of Rock Mechanics and Mining Sciences, 2013, 60: 389−400
3. Yang J H, Lu W B, Jiang Q H, Yao C, Zhou C B. Frequency comparison of blast-induced vibration per delay for the full-face millisecond delay blasting in underground opening excavation. Tunnelling and Underground Space Technology, 2016, 51: 189−201
4. Sastry V R, Chandra G R. Assessment of seismic energy obtained from blast induced ground vibrations using signal processing computation techniques. In: Processing of on Recent Trends in Electronics Information & Communication Technology. Bangalore: IEEE, 2016, 31−35
5. Hudaverdi T. Application of multivariate analysis for prediction of blast-induced ground vibrations. Soil Dynamics and Earthquake Engineering, 2012, 43: 300−308
6. Zhou J, Lu W, Yan P, Chen M, Wang G. Frequency-dependent attenuation of blasting vibration waves. Rock Mechanics and Rock Engineering, 2016, 49(10): 4061−4072
7. Li H, Li X, Li J, Xia X, Wang X. Application of coupled analysis methods for prediction of blast-induced dominant vibration frequency. Earthquake Engineering and Engineering Vibration, 2016, 15(1): 153−162
8. Deng X F, Zhu J B, Chen S G, Zhao Z Y, Zhou Y X, Zhao J. Numerical study on tunnel damage subject to blast-induced shock wave in jointed rock masses. Tunnelling and Underground Space Technology, 2014, 43: 88−100
9. Motoyama Y, Mikame S, Nojima K, Kawahara M. Second-order adjoint equation method for parameter identification of rock based on blast waves in tunnel excavation. Engineering Optimization, 2014, 46(7): 939−963
10. Li P, Lu W B, Wu X X, Chen M, Yan P, Hu Y G. Spectral prediction and control of blast vibrations during the excavation of high dam abutment slopes with millisecond-delay blasting. Soil Dynamics and Earthquake Engineering, 2017, 94: 116−124
11. Cohen A. Numerical Analysis of Wavelet Methods. Amsterdam: Elsevier, 2003
12. Morlet J, Arens G, Fourgeau E, Glard D. Wave propagation and sampling theory. Geophysics, 1982, 47(2): 203−221
13. Huang D, Cui S, Li X. Wavelet packet analysis of blasting vibration signal of mountain tunnel. Soil Dynamics and Earthquake Engineering, 2019, 117: 72−80
14. Ainalis D, Ducarne L, Kaufmann O, Tshibangu J P, Verlinden O, Kouroussis G. Improved analysis of ground vibrations produced by man-made sources. Science of the Total Environment, 2018, 616−617: 517−530
15. Wheeler R M. How millisecond delay periods may enhance or deduce blast vibration effects. Mining Engineering, 1988, 40(10): 969−973
16. Zhang Y P, Liu Z X. Wavelet analysis and Hilbert-Huang transform of blasting vibration signal. Explosion and Shock Waves, 2005, 25(6): 528−535
17. Lan M X, Lin C M. Wavelet packet analysis of vibration caused by high rock slope blasting. Nonferrous Metals (Mining Section), 2009, 61(2): 43−45
18. Xu C, Deng C. Investigating spectral behavior of tunnel blast induced vibration using wavelet analysis a case study of a dam in China. Journal of Civil Structural Health Monitoring, 2016, 6(3): 637−647
19. Hinzen K G. Comparison of seismic and explosive energy in five

smooth blasting test rounds. International Journal of Rock Mechanics and Mining Sciences, 1998, 35(7): 957−967

20. Ling T H, Li X B. Time-energy analysis based on wavelet transform for identifying real delay time in millisecond blasting. Chinese Journal of Rock Mechanics and Engineering, 2004, 23(12): 2266− 2270 (in Chinese)
21. Zhong G S, Li J, Zhao K. Structural safety criteria for blasting vibration based on wavelet packet energy spectra. Mining Science and Technology (China), 2011, 21(1): 35−40
22. Aldas G G U, Ecevitoglu B. Waveform analysis in mitigation of blast-induced vibrations. Journal of Applied Geophysics, 2008, 66(1−2): 25−30